

# Temperature-Programmed Precise Control over the Sizes of Carbon Nanospheres Based on Benzoxazine Chemistry

Shuai Wang, Wen-Cui Li, Guang-Ping Hao, Yan Hao, Qiang Sun, Xiang-Qian Zhang, and An-Hui Lu\*

State Key Laboratory of Fine Chemicals, School of Chemical Engineering, Dalian University of Technology, Dalian 116024, P.R. China

Supporting Information

**ABSTRACT:** On the basis of benzoxazine chemistry, we have established a new way to synthesize highly uniform carbon nanospheres with precisely tailored sizes and high monodispersity. Using monomers including resorcinol, formaldehyde, and 1,6-diaminohexane, and in the presence of Pluronic F127 surfactant, polymer nanospheres are first synthesized under precisely programmed reaction temperatures. Subsequently, they are pseudomorphically and uniformly converted to carbon nanospheres in high yield, due to the excellent thermal stability of such polybenzoxazine-based polymers. The correlation between the initial reaction temperature (IRT) and the nanosphere size fits well with the quadratic function model, which can in turn predict the nanosphere size at a set IRT. The nanosphere sizes can easily go down to 200 nm while retaining excellent monodispersity, i.e., polydispersity <5%. The particle size uniformity is evidenced by the formation of large areas of periodic assembly structure. NMR, FT-IR, and elemental analyses prove the formation of a polybenzoxazine framework. As a demonstration of their versatility, nanocatalysts composed of highly dispersed Pd nanoparticles in the carbon nanospheres are fabricated, which show high conversion and selectivity, great reusability, and regeneration ability, as evidenced in a selective oxidation of benzyl alcohol to benzaldehyde under moderate conditions.

The synthesis of highly uniform carbon nanospheres, particularly ones with particle sizes around or even below 200 nm, is extremely difficult and remains a grand challenge. In the fields of drug delivery,<sup>1</sup> biodiagnostics,<sup>2</sup> catalysis chromatography,<sup>3</sup> colloidal catalysts,<sup>4</sup> particle templates,<sup>5</sup> photonic crystals,<sup>6</sup> complex structures,<sup>6a</sup> and nanodevices,<sup>7</sup> strict control of the monodispersity and particle sizes <200 nm are necessary.<sup>8</sup> That has driven researchers to make long-term, unremitting efforts toward synthesizing such monodisperse carbon nanospheres. Although there are several reports on the synthesis of carbon microspheres and nanospheres from phenolic resins,<sup>9</sup> it is rare to find a report about truly monodisperse phenolic resin nanospheres whose sizes are <200 nm and so uniform that they can form three-dimensional periodic structures by self-assembly.<sup>9g</sup> For that, nanospheres with size distribution <5% are required.<sup>10</sup> Although colloidal nanospheres of polystyrene,<sup>5b,c,f</sup> poly(methyl methacrylate),<sup>11a</sup> and poly(hydroxyethyl methacrylate)<sup>11b</sup> are widely prepared with high monodispersity,<sup>7</sup> they failed to convert to carbons because of bad thermal stability. Hence, to achieve truly monodisperse carbon nanospheres, it is

key to explore new syntheses of polymer analogues that concurrently feature good thermal stability, high monodispersity, and heteroatoms in the framework, since carbons doped with heteroatoms have performed the best in many areas. They could then be converted to carbon nanospheres without deformation. The discovery of such carbon nanospheres with tightly controlled sizes and heteroatoms doping will provide powerful alternatives for the aforementioned applications.

Based on benzoxazine chemistry,<sup>12</sup> heterocyclic benzoxazine monomers are first generated by Mannich condensation of phenols, aldehydes, and amines without added initiators or catalysts; subsequently, polybenzoxazines are formed through thermally activated polymerization of the monomers.<sup>13</sup> The diversity of phenols, aldehydes, and amines that can be used offers remarkable flexibility in the molecular design of monomers; as a result, versatile, high-performance polymers can be expected. Inspired by the advanced properties of polybenzoxazines, including multireactive surfaces, low volumetric shrinkage, and remarkable thermal and mechanical stability,<sup>12</sup> we have ignited an effort to explore the synthesis of carbon-based materials based on this type of polymers.

Here we describe a new synthesis of highly uniform carbon nanospheres based on benzoxazine chemistry. It relies on first the successful creation of polybenzoxazine-based nanospheres (denoted PBFS) which can be transferred to carbon nanospheres, owing to their good thermal stability and high char yield. Their sizes can be precisely adjusted in the range of 95–225 nm by a straightforward temperature programming process. Moreover, PBFS itself can be an extraordinary building block for the preparation of colloidal Pd/carbon catalysts, showing high dispersion of Pd nanoparticles, high catalytic activity, great reusability, and regeneration ability in the selective oxidation of benzyl alcohol to benzaldehyde under moderate conditions. To the best of our knowledge, carbon nanospheres with such excellent properties have not been reported yet.

First, highly uniform polymer nanospheres with tunable sizes were synthesized through a solution-based process using resorcinol, formaldehyde, and 1,6-diaminohexane (DAH) as the monomers, together with Pluronic F127 surfactant. During the experiments, we noticed that the reaction takes place rapidly upon addition of DAH into the previously prepared solution resorcinol/formaldehyde/F127/water. For example, at an initial reaction temperature (IRT) of 24 °C, the reaction solution became white and opaque within 40 s, and much more so after 120 s (see Figure S1 in the Supporting Information (SI)); IRT is

Received: July 8, 2011

Published: September 05, 2011

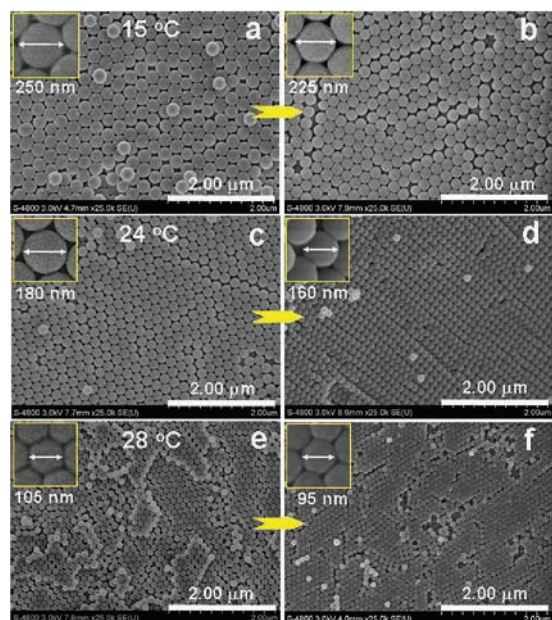


**Figure 1.** SEM images of the monodisperse polymer nanospheres PBFS-1, -2, and -3, prepared at different initial reaction temperatures, (a) 15, (c) 24, and (e) 28 °C, and their corresponding carbonized analogues CBFS (b,d,f).

defined as the temperature at which the reactants are mixed before being heated to the final reaction temperature of 80 °C). This reminds us to set a careful control on the reaction temperature in order to achieve nanospheres of tailorable particle sizes. From the heterogeneous nucleation and growth theory,<sup>14</sup> it is known that the number of nuclei formed is a function of temperature when other reaction conditions are identical. At higher temperatures, the effective surface energy is lower, thus diminishing the free energy barrier, facilitating nucleation, and forming more nuclei. Under such conditions, nuclei grow to smaller-size spheres in the particle growth stage. This indeed favors a highly uniform product. The scanning electron microscopy (SEM) images in Figure 1a,c,e suggest that the obtained PBFS polymer nanospheres show good colloid stability and uniformity in particle sizes (for dynamic light scattering data, see SI Figure S2). Interestingly, self-assembled periodic structures with close-packed planes arranged along the (111) direction are observed, indicating a good monodispersity of the obtained polymer nanospheres.<sup>15</sup>

Indeed, the sizes of the monodisperse nanospheres are remarkably affected by the IRT of the reactants. By carefully controlling the IRTs in the order of 15, 24, and 28 °C, the sizes of the resultant spheres, respectively denoted PBFS-1, -2, and -3, can be finely adjusted as  $250 \pm 6$ ,  $180 \pm 4$ , and  $105 \pm 5$  nm. That is, the sizes of the polymer nanospheres increase as the IRT decreases. It can be explained that a low IRT would slow the reaction rate, presumably initiating fewer nuclei in the reaction solution.<sup>16</sup> As a result, larger polymer nanospheres are formed as the reaction time progresses. Conversely, a high IRT would lead to a fast reaction rate and many nuclei in the solution; thus, smaller polymer nanospheres are formed as the time progresses. As can be seen in SI Figure S3, PBFS-1, -2, and -3 after centrifugation exhibit bright, shiny colors of red, green, and purple, respectively. This is additional proof that the obtained nanospheres are highly uniform in size. In contrast, when the IRT was increased to 40 °C, a three-dimensional network structure was obtained (see SI Figure S4a).

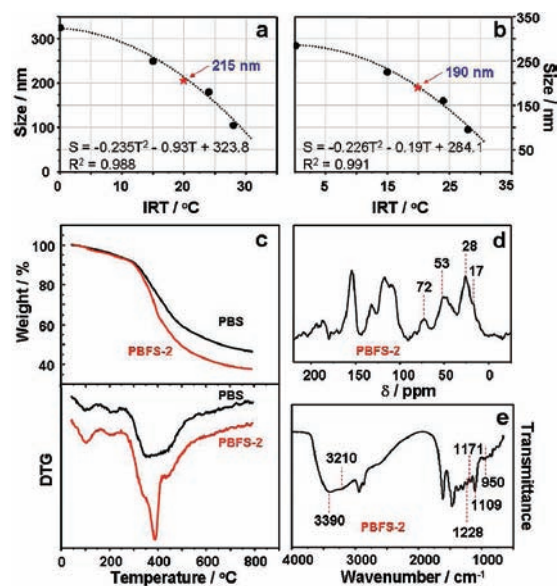


**Figure 2.** Relationship between the IRT and nanosphere sizes of PBFS (a) and CBFS (b). TG and DTG curves of PBFS-2 and PBS (prepared without F127 at the IRT of 24 °C) (c). <sup>1</sup>H→<sup>13</sup>C CP/MAS NMR (d) and FT-IR (e) spectra of PBFS-2.

This is due to the fast nucleation and growth of the primary polymeric particles, instead of the formation of nanospheres by minimizing the surface free energy.<sup>17</sup> We therefore speculated that lower IRTs would lead to nanospheres with even bigger sizes. Indeed, when the IRT was 0 °C, we obtained polymer nanospheres with a size of 325 nm (Figure S4c). We are thus certain that nanosphere size is temperature dependent. By using experimental data of IRT and nanosphere size with the polynomial fitting, a good quadratic function of size vs IRT is obtained (Figure 2a). Thus, the size of the polymer nanospheres can be, in turn, predicted by the quadratic function model. Additional experiments will verify the usability and accuracy of this model. For example, when the IRT was set as 20 °C, the calculated size of the polymer was 211 nm, while the experiment gave a sphere with a size of ~215 nm (SI Figure S5a); the simulated value agreed very well with the experiment result. Hence, our synthesis is validated to have the ability to achieve polybenzoxazine-based nanospheres with precisely controlled sizes through programming the IRT. The yields of the polymer nanospheres are typically 70–90%, depending on the synthesis conditions (see SI). Thanks to the diversity of the monomers that benzoxazine chemistry offers, one can envisage the generality and flexibility of our synthesis toward highly uniform polymer and carbon nanospheres. For example, when we replaced DAH with other amines, such as 1,2-diaminoethane, and followed the synthesis conditions of PBFS-2, polymer nanospheres with uniform sizes were obtained as well (see representative SEM images in SI Figure S6).

Importantly, pyrolysis of the polymer nanospheres at 500 °C gives carbon nanospheres denoted as CBFS-1, -2, and -3, corresponding to the polymer analogues PBFS-1, -2, and -3. The BET surface areas of CBFS-1, -2, and -3 are respectively 382, 422, and 407 m<sup>2</sup> g<sup>-1</sup>. As shown in Figure 1b,d,f, they retain perfect spherical shape and high uniformity in sizes. Like their polymer analogues, the sizes of carbon nanospheres are also temperature dependent (Figures 2b and S5b). The volume contraction of CBFS-1, -2, and -3 after thermal treatment is respectively 27.1,



29.8, and 25.9%, while the linear shrinkage is 10.0, 11.1, and 9.5%. Apparently, the thermal shrinkage of such nanospheres is independent of their size. This proves the excellent structural homogeneity and great thermal stability of such polybenzoxazine-based nanospheres. To show the excellent homogeneity of the carbon sample, a typical SEM image recorded on a large area of CBFS-2 is provided in SI Figure S7.

To check the thermal behavior of the polymer nanospheres, TG-DTG analysis was conducted for PBFS-2 as an example. For comparison, polymer prepared without F127 at the IRT of 24 °C (denoted PBS) was analyzed as a control sample. As shown in Figure 2c, the TG curve of PBFS-2 exhibits ~38% of the residual carbon at 800 °C, whereas polymer PBS displays a carbon conversion of 46%. Such a high carbon yield indicates this polymer is an excellent precursor for the production of carbonaceous material.<sup>13</sup> The differences between the two samples can be ascribed to the use of F127 in the synthesis. Based on the TG results, a roughly estimated amount of F127 is ~8 wt %. During this study we found that F127 is indispensable and ensures the formation of nanosized monodisperse polymer spheres. The same experiment was carried out without F127, leading to a product comprised of large polymer spheres of 650–700 nm (see Figure S4b). It should be mentioned that, in this synthesis, surfactant F127 most likely acts as an interface stabilizing agent rather than a template. The DTG curves of these two samples display a big difference of sharp weight loss at ~390 °C, attributed to the decomposition of F127 present in the nanospheres.<sup>18</sup> Furthermore, incorporation of F127 in PBFS-2 was confirmed by <sup>1</sup>H→<sup>13</sup>C CP/MAS NMR analysis (Figure 2d), showing signals at ~72 and 17 ppm that correspond to the carbons in the methylene and methyl groups of the Pluronic F127. Thus, the nonwashable F127 content is supposed to be the amount entrapped in the PBFS when the surfactant acts as an emulsion agent. The resolved peaks at ~53 and 28 ppm are the signals of the methylene groups in Ar–CH<sub>2</sub>–N and –(CH<sub>2</sub>)<sub>6</sub>–, respectively. In addition, the FTIR spectrum of PBFS-2 (Figure 2e) shows a band at ~1171 cm<sup>-1</sup>, which can be assigned to C–N stretching; the strongest hydrogen-bonded hydroxyl bands at ~3210 and 3390 cm<sup>-1</sup> can be assigned to –OH···N intramolecular hydrogen bonding in the Mannich bridge and –OH···π hydrogen bonding,<sup>13a,b</sup> respectively, indicative of the abundant hydroxyl groups produced during ring-opening polymerization of benzoxazine. The stretching of the aromatic ether at ~1109 and 1228 cm<sup>-1</sup> and the weak band at ~950 cm<sup>-1</sup> originate from the benzene ring to which oxazine is attached, revealing the characteristics of the benzoxazine residues in the as-made polybenzoxazines (see SI Figure S8). Hence, the NMR and IR results verify that the resultant polymer product is a kind of polybenzoxazine. In addition, elemental analysis confirms that both the PBFS and the CBFS exhibit high contents of nitrogen, ~3.7 and ~2.2 wt %, respectively. This is another strong indication of nitrogen heteroatom incorporation into the carbon framework.

It is easy to imagine that such uniform nanospheres can be used in catalysis, drug delivery, building complex structures, nanocasting, and electrochemistry. In the following, we demonstrate one such application. Nanocatalysts consisting of Pd nanoparticles dispersed in the carbon nanospheres were prepared by complexing Pd<sup>2+</sup> (H<sub>2</sub>PdCl<sub>4</sub> aqueous solution) into PBFS-2, followed by thermal treatment at 500 °C. The loading amount of Pd is ~1 wt %. Pd-catalyzed oxidation of benzyl alcohol to benzaldehyde was chosen as a model reaction to evaluate the catalytic activity of the Pd@CBFS-2 nanocatalyst. Transmission electron

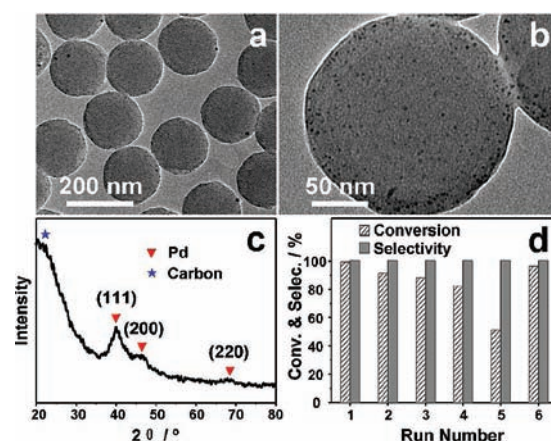


**Figure 3.** TEM images (a,b) and XRD pattern (c) of the colloidal catalyst Pd@CBFS-2 pyrolyzed at 500 °C. Conversion and selectivity (d) of the recycled and regenerated Pd@CBFS-2 catalyst for benzyl alcohol selective oxidation.

microscopy (TEM) of this nanocatalyst (Figure 3a,b) shows that most of the Pd nanoparticles with sizes of 2.5–3.5 nm are highly dispersed in the carbon matrix. X-ray diffraction of Pd@CBFS-2 (Figure 3c) shows very low intensity reflections resulting from metallic Pd, indicating that the Pd particles are small. This is also consistent with the TEM observations.

The catalytic reactions were carried out under moderate reaction conditions: ambient pressure, 80 °C, and water as the “green” solvent. The results show that such a catalyst exhibits an extremely high conversion (99%) with high selectivity to benzaldehyde (>99%) in 2 h in aqueous solution under oxygen ambient. In comparison to bulky heterogeneous catalysts under similar reaction conditions,<sup>19</sup> the nanocatalyst exhibits a fast reaction rate, showing higher turnover frequency due to the easy accessible active Pd sites and high selectivity (see SI Table S1 for the comparison). This is due to the porosity of the carbon matrix (see SI Figure S9) and the surface-located Pd sites. Investigation of the recyclability of the Pd@CBFS-2 catalyst showed excellent results in a total of four cycles (Figure 3d), i.e., high selectivity (>99%) and conversion (>82%). The fifth cycle still gave high selectivity (>99%) but a drop in conversion (51%). No detectable acid was found in the product, indicating that the alcohol was selectively converted to aldehyde. These properties were superior to those observed for the reported Pd/C catalysts<sup>19</sup> (see Table S1). To determine if Pd nanoparticles are lost during the reaction, the partially reacted solution after the fifth cycle was centrifuged to remove the Pd@CBFS-2 catalyst, and the supernatant solution together with a certain amount of fresh benzyl alcohol was transferred to a new reactor. However, even after 8 h, no benzyl alcohol consumption was detected. This experiment proves the good stability of our colloidal catalyst. Surprisingly, the catalyst can be easily regenerated by a simple calcination treatment at 200 °C under air to clean the adsorbed organic species from the surface of Pd nanoparticles.<sup>20</sup> After heat treatment, this catalyst recovers its activity of high conversion (>96%) and selectivity (>99%), as shown in Figure 3d (run 6). These results confirm the high catalytic activity, great reusability, and regeneration ability of this nanocatalyst.

In summary, we have developed a new synthesis based on benzoxazine chemistry that leads to temperature-programmed precise control over the size of targeted carbon nanospheres. It

was found that the IRT predicted the nanosphere size following the quadratic function model. Particles as small as ~95 nm can be prepared with high monodispersity, as evidenced by the formation of an assembled periodic structure which strongly indicates the polydispersity to be <5%.<sup>10</sup> To our knowledge, this is the first successful synthesis of highly uniform, polybenzoxazine-based, nanometer-sized spheres. Such nanospheres can be used as nanocatalysts with high catalytic activity, great reusability, and regeneration ability. This new type of nanocatalysts is expected to generally show long catalyst lifetime in reactions catalyzed by various noble metals. Thanks to the diverse options of monomers for polybenzoxazines, our synthesis strategy may provide a highly efficient process for the preparation of a wide range of polybenzoxazine-based nanospheres, which can readily undergo subsequent functionalization and processing. We expect that this finding will have a considerable impact on the development of advanced carbon nanospheres for applications in catalysis, drug delivery, building complex structures, nanocasting, electrochemistry, and adsorption.

## ■ ASSOCIATED CONTENT

**S Supporting Information.** Experimental details and characterization data. This material is available free of charge via the Internet at <http://pubs.acs.org>.

## ■ AUTHOR INFORMATION

**Corresponding Author**  
anhuilu@dlut.edu.cn

## ■ ACKNOWLEDGMENT

The project was supported by NSFC (No. 20873014 and 21073026), the Program for New Century Excellent Talents in University of China (NCET-08-0075, NCET-09-0254), the Scientific Research Foundation for the Returned Overseas Chinese Scholars, State Education Ministry, and the Ph.D. Programs Foundation (20100041110017) of Ministry of Education of China. We thank Prof. X. Pan and Dr. W. Shen at DICP for measuring NMR.

## ■ REFERENCES

- (1) (a) Hong, S. H.; Moon, J. H.; Lim, J. M.; Kim, S. H.; Yang, S. M. *Langmuir* **2005**, *21*, 10416–10421. (b) Kim, J.; Kim, H. S.; Lee, N.; Kim, T.; Kim, H.; Yu, T.; Song, I. C.; Moon, W. K.; Hyeon, T. *Angew. Chem., Int. Ed.* **2008**, *47*, 8438–8441. (c) Liu, J.; Qiao, S. Z.; Hartono, S. B.; Lu, G. Q. *Angew. Chem., Int. Ed.* **2010**, *49*, 4981–4985.
- (2) Park, H.; Yang, J.; Seo, S.; Kim, K.; Suh, J.; Kim, D.; Haam, S.; Yoo, K. H. *Small* **2008**, *4*, 192–196.
- (3) Lin, C.; Li, Y.; Yu, M.; Yang, P.; Lin, J. *Adv. Funct. Mater.* **2007**, *17*, 1459–1465.
- (4) (a) Mihalcik, D. J.; Lin, W. B. *Angew. Chem., Int. Ed.* **2008**, *47*, 6229–6232. (b) Sun, X. M.; Li, Y. D. *Angew. Chem., Int. Ed.* **2004**, *43*, 597–601. (c) Cui, R. J.; Liu, C.; Shen, J. M.; Gao, D.; Zhu, J. J.; Chen, H. Y. *Adv. Funct. Mater.* **2008**, *18*, 2197–2204. (d) Tang, S. C.; Vongehr, S.; Meng, X. K. *J. Phys. Chem. C* **2010**, *114*, 977–982. (e) Bradley, C. A.; Yuhua, B. D.; McMurdo, M. J.; Tilley, T. D. *Chem. Mater.* **2009**, *21*, 174–185. (f) Kim, J.; Park, S.; Lee, J. E.; Jin, S. M.; Lee, J. H.; Lee, I. S.; Yang, I.; Kim, J. S.; Kim, S. K.; Cho, M. H.; Hyeon, T. *Angew. Chem., Int. Ed.* **2006**, *45*, 7754–7758. (g) Ge, J. P.; Zhang, Q.; Zhang, T. R.; Yin, Y. D. *Angew. Chem., Int. Ed.* **2008**, *47*, 8924–8928. (h) Deng, Y. H.; Cai, Y.; Sun, Z. K.; Liu, J.; Liu, C.; Wei, J.; Li, W.; Wang, Y.; Zhao, D. Y. *J. Am. Chem. Soc.* **2010**, *132*, 8466–8473.

- (5) (a) Yokoi, T.; Sakamoto, Y.; Terasaki, O.; Kubota, Y.; Okubo, T.; Tatsumi, T. *J. Am. Chem. Soc.* **2006**, *128*, 13664–13665. (b) Bartlett, P. N.; Birkin, P. R.; Ghanem, M. A.; Toh, C. S. *J. Mater. Chem.* **2001**, *11*, 849–853. (c) Yi, G. R.; Moon, J. H.; Yang, S. M. *Chem. Mater.* **2001**, *13*, 2613–2618. (d) Velev, O. D.; Jede, T. A.; Lobo, R. F.; Lenhoff, A. M. *Chem. Mater.* **1998**, *10*, 3597–3602. (e) Hu, J.; Abdelsalam, M.; Bartlett, P.; Cole, R.; Sugawara, Y.; Baumberg, J.; Mahajan, S.; Denuault, G. *J. Mater. Chem.* **2009**, *19*, 3855–3858. (f) Kim, M. H.; Im, S. H.; Park, O. O. *Adv. Funct. Mater.* **2005**, *15*, 1329–1335. (g) Holland, B. T.; Blanford, C. F.; Stein, A. *Science* **1998**, *281*, 538–540. (h) Yan, H. W.; Blanford, C. F.; Smyrl, W. H.; Stein, A. *Chem. Commun.* **2000**, 1477–1478. (i) Li, F.; Josephson, D. P.; Stein, A. *Angew. Chem., Int. Ed.* **2011**, *50*, 360–388.
- (6) (a) Jeong, U.; Wang, Y. L.; Ibisate, M.; Xia, Y. N. *Adv. Funct. Mater.* **2005**, *15*, 1907–1921. (b) Wang, Y. J.; Price, A. D.; Caruso, F. *J. Mater. Chem.* **2009**, *19*, 6451–6464. (c) Xia, Y. N.; Gates, B.; Yin, Y. D.; Lu, Y. *Adv. Mater.* **2000**, *12*, 693–713.
- (7) Galisteo-López, J. F.; Ibisate, M.; Sapienza, R.; Froufe-Pérez, L. S.; Blanco, Á.; López, C. *Adv. Mater.* **2011**, *23*, 30–69.
- (8) (a) Xiang, S. D.; Scholzen, A.; Minigo, G.; David, C.; Apostolopoulos, V.; Mottram, P. L.; Plebanski, M. *Methods* **2006**, *40*, 1–9. (b) Gu, J. L.; Su, S. S.; Li, Y. S.; He, Q. J.; Shi, J. L. *Chem. Commun.* **2011**, 2101–2103.
- (9) (a) Fang, Y.; Gu, D.; Zou, Y.; Wu, Z. X.; Li, F. Y.; Che, R. C.; Deng, Y. H.; Tu, B.; Zhao, D. Y. *Angew. Chem., Int. Ed.* **2010**, *49*, 7987–7991. (b) Long, D. H.; Lu, F.; Zhang, R.; Qiao, W. M.; Zhan, L.; Liang, X. Y.; Ling, L. C. *Chem. Commun.* **2008**, 2647–2649. (c) Friedel, B.; Greulich-Weber, S. *Small* **2006**, *2*, 859–863. (d) Dong, Y. R.; Nishiyama, N.; Egashira, Y.; Ueyama, K. *Ind. Eng. Chem. Res.* **2008**, *47*, 4712–4716. (e) Scherdel, C.; Scherb, T.; Reichenauer, G. *Carbon* **2009**, *47*, 2244–2252. (f) Lu, A. H.; Li, W. C.; Hao, G. P.; Spliethoff, B.; Bongard, H. J.; Schaack, B. B.; Schüth, F. *Angew. Chem., Int. Ed.* **2010**, *49*, 1615–1618. (g) Liu, J.; Qiao, S. Z.; Liu, H.; Chen, J.; Orpe, A.; Zhao, D. Y.; Lu, G. Q. *Angew. Chem., Int. Ed.* **2011**, *50*, 5947–5951.
- (10) Jiang, P.; Bertone, J. F.; Colvin, V. L. *Science* **2001**, *291*, 453–457.
- (11) (a) D'Amato, R.; Venditti, I.; Russo, M. V.; Falconieri, M. *J. Appl. Polym. Sci.* **2006**, *102*, 4493–4499. (b) Pan, G. S.; Tse, A. S.; Kesavamoorthy, R.; Asher, S. A. *J. Am. Chem. Soc.* **1998**, *120*, 6518–6524.
- (12) (a) Ghosh, N. N.; Kiskan, B.; Yagci, Y. *Prog. Polym. Sci.* **2007**, *32*, 1344–1391. (b) Yagci, Y.; Kiskan, B.; Ghosh, N. N. *J. Polym. Sci., Part A: Polym. Chem.* **2009**, *47*, 5565–5576.
- (13) (a) Chernykh, A.; Liu, J. P.; Ishida, H. *Polymer* **2006**, *47*, 7664–7669. (b) Allen, D. J.; Ishida, H. *Polymer* **2007**, *48*, 6763–6772. (c) Baqar, M.; Agag, T.; Ishida, H.; Qutubuddin, S. *Polymer* **2011**, *52*, 307–317. (d) Agag, T.; Arza, C. R.; Maurer, F. H. J.; Ishida, H. *Macromolecules* **2010**, *43*, 2748–2758. (e) Nakamura, M.; Ishida, H. *Polymer* **2009**, *50*, 2688–2695. (f) Wang, C. F.; Su, Y. C.; Kuo, S. W.; Huang, C. F.; Sheen, Y. C.; Chang, F. C. *Angew. Chem., Int. Ed.* **2006**, *45*, 2248–2251.
- (14) (a) Song, J. S.; Tronc, F.; Winnik, M. A. *J. Am. Chem. Soc.* **2004**, *126*, 6562–6563. (b) Tseng, C. M.; Lu, Y. Y.; El-Aasser, M. S.; Vanderhoff, J. W. *J. Polym. Sci., Part A: Polym. Chem.* **1986**, *24*, 2995–3007.
- (15) (a) Agrawal, M.; Fischer, D.; Gupta, S.; Zafeiropoulos, N. E.; Pich, A.; Lidorikis, E.; Stamm, M. *J. Phys. Chem. C* **2010**, *114*, 16389–16394. (b) Zhang, J. H.; Li, Y. F.; Zhang, X. M.; Yang, B. *Adv. Mater.* **2010**, *22*, 4249–4269.
- (16) Yano, K.; Fukushima, Y. *J. Mater. Chem.* **2003**, *13*, 2577–2581.
- (17) Chen, Q. R.; Han, L.; Gao, C. B.; Che, S. N. *Microporous Mesoporous Mater.* **2010**, *128*, 203–212.
- (18) Lu, A. H.; Spliethoff, B.; Schüth, F. *Chem. Mater.* **2008**, *20*, 5314–5319.
- (19) (a) Dimitratos, N.; Villa, A.; Wang, D.; Porta, F.; Su, D.; Prati, L. *J. Catal.* **2006**, *244*, 113–121. (b) Villa, A.; Janjic, N.; Spontoni, P.; Wang, D.; Su, D.; Prati, L. *Appl. Catal. A* **2009**, *364*, 221–228.
- (20) (a) Harada, T.; Ikeda, S.; Hashimoto, F.; Sakata, T.; Ikeue, K.; Torimoto, T.; Matsumura, M. *Langmuir* **2010**, *26*, 17720–17725. (b) Mallat, T.; Baiker, A. *Chem. Rev.* **2004**, *104*, 3037–3058.